Volume 13, Issue 1, Page 133-141, 2024 https://doi.org/10.46810/tdfd.1438617 Research Article

BİNGÖL UNIVERSITY

Türk Doğa ve Fen Dergisi
Turkish Journal of Nature and Science
www.dergipark.gov.tr/tdfd

Investigation of Mechanical Properties of Graphene-CNT Reinforced Nickel Metal Matrix Nanocomposite Structure

Ünal DEĞIRMENCI[1*]

[1] Bingöl University, Department of Machinery and Metal Technologies, Bingöl, Türkiye
Ünal DEĞİRMENCİ ORCID No: 0000-0003-1480-2488

**Corresponding author: udegirmenci@bingol.edu.tr*

(Received: 16.02.2024, Accepted: 17.03.2024, Online Publication: 26.03.2024)

Keywords
Nickel, Carbon-based nanomaterials, Mechanical properties, Molecular dynamics simulations

Abstract: Nickel is a metal widely used in many industrial applications, but despite its superior properties, it also has some shortcomings. Carbon-based structures can be important reinforcement elements in improving the properties of metals. By providing a balance between the high corrosion resistance, high electrical conductivity and good magnetic properties of the nickel material and the lightness and high strength of carbon-based structures, a material with advanced properties can be obtained. Therefore, in this study, a new Nickel-Carbon nanostructure supported by a covalently bonded graphene-carbon nanotube (CNT) skeleton structure is presented. Additionally, it was aimed to investigate the mechanical properties and deformation mechanisms in all directions by designing three materials with different geometric dimensions (Ni-G-CNT(5,5), Ni-G-CNT(10,10) and Ni-G-CNT(15,15)). According to the results, it was observed that G-CNT structures increased the tensile and compressive behavior of the Ni structure in the CNT direction. With the addition of G-CNT structures, a 36% increase in the elastic modulus of the nickel structure and a 12% increase in the maximum tensile value were observed. For tensile loading in the CNT direction, as the CNT diameter decreases, the elastic modulus of the hybrid structures increases, while the maximum stress values are independent of the CNT diameter. As the CNT diameter increases, the ductility of the structures increases. In terms of compressive strength, it has been observed that in the linear region, as the CNT diameter increases, the strength generally increases and in the condensation region, it exhibits better compressive strength. With this study, an anisotropic nanostructure that is lighter and can exhibit higher mechanical strength compared to the Nickel structure is presented.

Grafen-CNT Takviyeli Nikel Metal Matrisli Nanokompozit Yapının Mekanik Özelliklerinin İncelenmesi

Anahtar Kelimeler
Nikel, Karbon bazlı nanomalzemeler, Mekanik özellikler, Moleküler dinamik simülasyonları

Öz: Nikel, birçok endüstriyel uygulamada yaygın olarak kullanılan bir metaldir, ancak üstün özelliklerinin yanı sıra bazı eksik yanları da mevcuttur. Metallerin özelliklerini iyileştirmede karbon temelli yapılar önemli takviye elemanı özelliği gösterirler. Nikel malzemesinin yüksek korozyon direnci, elektrik iletkenliği ve iyi manyetik özelliği ile karbon bazlı yapıların hafiflik ve yüksek mukavemeti arasında bir denge sağlayan gelişmiş özelliklere sahip bir malzeme elde edilebilir. Bu nedenle, bu çalışmada, kovalent olarak bağlı grafen-karbon nanotüp (KNT) iskelet yapısı ile desteklenmiş yeni bir nikel-karbon nanoyapısı sunulmaktadır. Ayrıca, farklı geometrik boyutlara sahip üç malzeme tasarımı (Ni-G-CNT(5,5), Ni-G-CNT(10,10) ve Ni-G-CNT(15,15)) yapılarak yapıların tüm doğrultulardaki mekanik özellikleri ve deformasyon mekanizmaları araştırmıştır. Sonuçlara göre, G-CNT yapılarının Ni yapısının çekme ve basma davranışını KNT doğrultusunda artırdığı görülmüştür. G-CNT yapılarının eklenmesi ile nikel yapısının elastik modülü değerinde %36, maksimum gerilme değerinde ise %12 artış gözlenmiştir. KNT doğrultusunda çekme yüklemeleri için KNT çapı azaldıkça hibrit yapıların elastik modülü artarken maksimum gerilme değerleri KNT çapından bağımsızdır. KNT çapı arttıkça ise yapıların süneklikleri artmaktadır. Basma dayanımı açısından ise lineer bölgede genel olarak KNT çapı arttıkça dayanımın arttığı yoğunlaşma bölgesinde ise daha iyi basma dayanımı sergilediği görülmüştür. Bu çalışma ile Ni yapısına kıyasla daha hafif ve daha yüksek mekanik dayanım sergileyebilen anizotropik bir nanoyapı sunulmuştur.

1. INTRODUCTION

Today, materials science and engineering form the basis of advanced technologies and innovative applications. In this field, improving and optimizing the properties of materials is vital to improving performance in various industries. In this context, hybrid nanocomposites have attracted great attention from researchers in recent years. Metal matrix nanocomposites have an important place in this field[1]. Among metals, nickel is very important due to its rust resistance, high temperature and chemical resistance, improved electrical conductivity and magnetic properties [2, 3]. Due to these properties, it is used in many areas such as automotive, shipbuilding, maritime, chemical industry, electric motors, magnetic sensors and power plants [4, 5]. Despite the many good properties of nickel material, its mechanical strength is not at the desired level [6]. For this reason, there is a need to strengthen it with various reinforcement materials.

Many materials are used as reinforcement materials in metal matrix nanocomposites [7, 8]. Among these, nanoscale materials such as graphene and CNT (Carbon Nanotube) have the potential to provide excellent reinforcement in composite materials because they have unique mechanical, electrical and thermal properties [9-12]. Some studies indicate that there is a potential to form a strong bond between carbon-based structures and some metals such as Ni, Pt, Pd and Ti [13, 14]. When nickel metal is combined with CNTs and graphene, a nickel matrix composite can be obtained, which is important for many applications. For this reason, there are various studies in the literature about carbon-based structures and nickel. For example; Jiang and his team[15], synthesized CNT/Ni hybrid nanostructure arrays using one-step chemical vapor deposition method (CVD). The study has shown that these structures can be used as high-performance capacitor materials thanks to their large area capacitance and superior rate capacitance. In another study, Wang et al. [16] investigated the effects of Ni-MWCNTs with different aspect ratios on the uniaxial tensile behavior of ultra-high strength concrete (UHPC) by experimental and MD analyses. The results obtained showed that the presence of Ni-MWCNTs markedly changed the tensile performances of UHPC.

Producing nanostructures and investigating their properties experimentally is a very expensive and difficult process. For this reason, using the Molecular Dynamics (MD) method provides a great advantage when investigating the properties of these structures [17, 18]. Molecular dynamics simulations are a powerful tool for studying material behavior at the atomic level. This method allows modeling of material behavior, taking into account atomic interactions and material properties. If we look at some studies conducted in this context; Zhou et al. [6] investigated the mechanical properties of nanoporous nickel and carbon nanotube (CNT) reinforced composites using molecular dynamics (MD) simulations at 900K. It was found that out-of-plane mechanical behavior were better than in-plane properties and CNT reinforcement increased the elastic modulus, tensile strength and compressive strength while decreasing the weight of the composites. Song and Zha [19] examined the behavior of nickel-plated single-wall CNTs and their gold matrix composites under axial loading using MD simulations. As a result, they found that although nickel plating reduced the tensile strength, nickel-CNT reinforcement could increase the Young's modulus of the composite. Yan et al. [20] investigated the mechanical properties of CNTs with different geometric properties embedded in the nickel matrix. They investigated the effects of CNT rotation angle, CNT number and CNT length on the deformation mechanism, ultimate tensile strength (UTS) and Young's modulus. It has been observed that the distribution of long and short CNTs significantly affects the Young's modulus and UTS of CNT/Ni nanocomposites, and the number of CNTs increases these properties.

There are some studies in the literature on composite materials obtained by combining graphene and CNT structures with nickel material. However, although the single effects of graphene and CNT have been mostly studied, there are no studies in which they are used together. For this reason, in this study, the Nickel nanocomposite structure supported by the G-CNT skeleton structure obtained by covalently bonding graphene to the CNT side walls was modeled with MD simulations and its mechanical properties were investigated. This new carbon-metal hybrid nanostructure is called Ni-G-CNT (Nickel-Graphene-CNT). In addition, in this study, three models with different G-CNT skeletons (G-CNT(5, 5), G-CNT(10, 10), and G-CNT(15, 15)) were created by keeping the carbon density constant and their mechanical behaviors such as tensile and compression were compared. It is thought that the results will make a significant contribution to the design and production of more durable, lightweight and high-performance materials. Additionally, this composite has the potential to be used in structural components in the aerospace, automotive and aerospace industries.

2. MATERIAL AND METHOD

2.1. Atomistic Modeling

The Ni-G-CNT hybrid structures proposed in this study consist of a Nickel matrix nanocomposite structure reinforced with graphene-CNT skeleton covalently bonded together along the CNT. Atomic models of the relevant nanostructures were created in three steps. In the first step, the atomic coordinates of graphenes (GNRs) and carbon nanotubes (CNTs) were created separately using Visual Molecular Dynamics (VMD) [21] software. In the second step, a certain number of graphene sheets were placed along the outer surface of the CNTs and a G-CNT skeleton was formed by creating a covalent bond between the graphene and CNT structures with the help of thermal welding process. In the next stage, the G-CNT skeleton structure was embedded in the nickel matrix and the atomic model of the Ni-G-CNT structures was obtained. After the coordinates of the nanostructures are created, they are minimized and stabilized at room temperature (300 K) and their stability is examined. The diagram of the modeling process of hybrid nanostructures is shown in Figure 1.

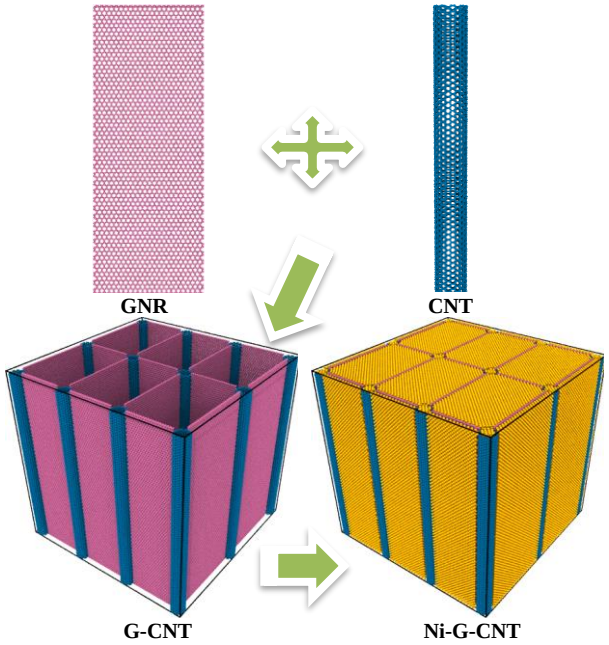

Figure 1. Schematic representation of the modeling process of Ni-G-CNT structures.

In this study, three different Ni-G-CNT structures containing different G-CNT types (G-CNT(5, 5), G-CNT(10, 10), and G-CNT(15, 15)) with equal lengths and CNTs of different diameters containing approximately a fixed number of carbons were created. In order to provide approximately equal carbon atom density, the size of graphene and the number of CNTs vary depending on the models. The dimension and numbers of the carbon nanotubes and graphene used in the structures are given in Table 1.

Table 1. Dimension and atomic numbers of graphene and CNTs in models.

Models		Ni-G-CNT(5,5)	Ni-G-CNT(10,10)	Ni-G-CNT(15,15)
CNT Type		(5,5)	(10,10)	(15,15)
CNT Diameters (nm)		0.6808	1.3560	2.0324
Graphene Dimensions(nm)	Y	5.5x20	7.5x20	6.44x20
	X	5.5x20	4.5x20	3.5x20
CNT Numbers		16	12	12
GNR Numbers		24	17	17

To create G-CNT structures, it is necessary to create covalent bonds between graphene plates and CNTs. This process is carried out by the thermal welding method, which is an annealing process [22, 23]. In this annealing process, graphene sheets are aligned to the CNT side walls. Then, by applying high temperatures to the boundaries of CNT and graphene, bonds break in the structures and new bonds are formed between graphene and CNT. High temperatures are required to ensure bond formation during the thermal welding process. In order to save time and cost by performing this process in a lower temperature and time range, partial deformations are created in the atoms on the CNT side surfaces corresponding to the side surfaces of the graphene sheets. In this way, it is possible to create new ligaments more easily with the sagging ligaments created. Sample representations of Ni-G-CNT structures can be seen in Figure 2.

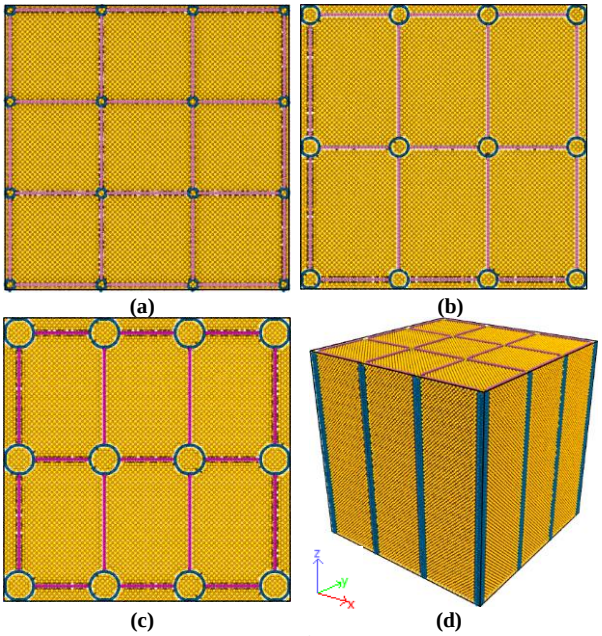

Figure 2. Sample representations of Ni-G-CNT structures; (a) Ni-G-CNT(5,5), (b) Ni-G-CNT(10,10), (c) Ni-G-CNT(15,15), (d) 3D image of Ni-G-CNT(5,5).

2.2. Simulation Details

MD simulations for the thermal welding process and mechanical analysis are performed using the open source Large Scale Atomic/Molecular Massively Parallel Simulator (LAMMPS) [24]. MD simulations provide interactions between atoms using interatomic potentials to calculate material behavior. In this study, hybrid potential was used for the interaction between atoms. In this context, the Adaptive Molecular Reactive Empirical Boundary Series (AIREBO) potential is used for the carbon atom interaction between graphene and CNT[25, 26]. The AIREBO potential is an important potential that can represent a dynamic system as it can accurately predict the formation of new bonds. The Embedded Atom Method (EAM) is used for force calculations between nickel atoms[27, 28]. Lennard jones potential is used for hybrid interactions between nickel and carbon atoms [29-31]. In the thermal welding procedure, the Nosé-Hoover thermostat and the canonical ensemble (NVT) system were used as thermodynamic properties to ensure the thermal balance of the system. The time step of the simulation was determined as 0.001 picoseconds (ps). Periodic boundary conditions are defined in all directions for the system to represent a large material structure.

The sintering temperature of nickel metal and the temperature values (1200 K) required to form covalent bonds between graphene and CNTs are very close to each other. For this reason, the thermal welding process is applied simultaneously to graphene and CNT atoms. In the thermal welding process, first the environment is kept

at 300 K for 50 picoseconds (ps) to achieve thermal equilibrium. Then, the temperature of the atoms in the region is gradually increased to the reference temperature of 1200 K with a temperature increase of 300 K. Energy is needed for both the sintering process and the breaking of bonds in CNTs and the formation of bonds with graphene. To provide this energy, the ambient temperature is kept constant at 1200K for 60 ps. Then, fractional cooling is performed to reduce the temperature of the region from 1200 K to 300 K within 50 ps. Finally, it is relaxed for 50 ps at 300 K. Thus, the stability of the bonds in the connection regions is examined [32]. The bonds formed between CNTs and graphene at the end of the thermal welding process are shown in Figure 3.

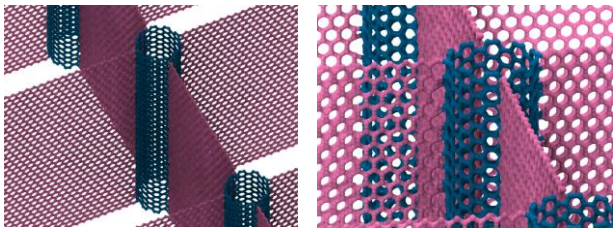

(a) (b)

Figure 3. Covalent bonds formed between CNT and graphene layers, a) bond view, b) close bond view.

Once the atomic models are created, the free energy profiles are monitored for 100 ps at room temperature to observe their thermal stability. For this process, it is thermalized at room temperature using the Nose-Hoover thermostat and NPT assembly. Mechanical tensile and compression analyzes were carried out by selecting the loading rate of 0.001 ps−1, which is widely used in the literature, and equilibrated at room temperature with NVT integration. Tensile analyzes were carried out separately in all three directions (X, Y, Z) to calculate the Elastic modulus (E), yield stress (σy) and ultimate stress (σu) values of the material and compare them with each other. Compression analyzes were carried out only in the CNT direction (Z), which is thought to exhibit the best behavior of the material. The atomistic stresses used to generate the stress-strain curves are calculated using the Virial stress theorem[33].

3. RESULTS AND DISCUSSION

In this study, firstly, the energy profiles were examined at 300 K for a sufficiently long time to examine whether the nanostructures were thermodynamically stable. It is seen that the energy values of the proposed structures remain almost constant. Additionally, there is no significant structural change in the structures compared to the initial design, indicating that they are thermodynamically stable. After it was understood that the structures were stable, mechanical tests were carried out.

3.1. Tensile Behavior

In this study, the tensile strengths of Ni-G-CNT structures supported by nickel and three G-CNT nanoskeleton system with different CNT diameters in each direction were analyzed by MD simulations under uniaxial loading. Since the structure has an anisotropic structure in terms of model, it exhibits different mechanical properties in each direction. The stress-strain graph of the structures obtained from the analysis results in the z-axis direction is given in Figure 4.

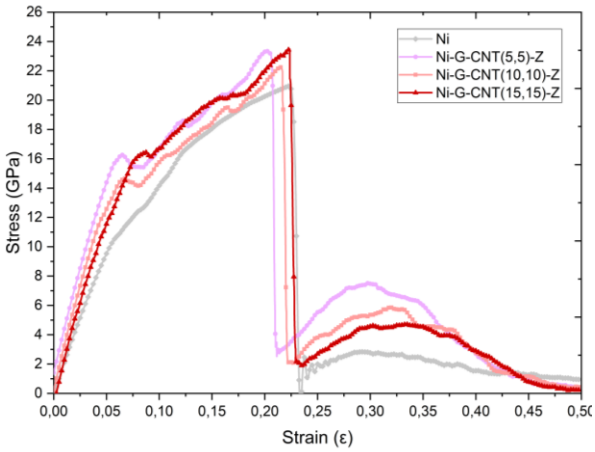

Figure 4. Tensile stress-strain curves of Ni-G-CNT structures in the z direction.

When the stress strain values in the CNT direction of the structures given in Figure 4 are examined, it is seen that with the addition of the G-CNT structure to the Ni structure, the mechanical properties increase with a partial decrease in the ductility of the nickel structure. When the mechanical behaviors of the structures are compared within themselves, the highest value in this direction belongs to the [CNT (5,5)] Ni-G-CNT(5,5) structure containing small diameter CNTs. The addition of carbon structures increased the tensile behavior of the structures in the linear region. It has been observed that as the CNT diameter increases, the elastic modulus and yield stress values of the structures decrease, but they still have high values compared to the Nickel structure. Although there was a regularly decreasing relationship between mechanical properties and increasing CNT diameter in the linear region, no regular relationship was found between CNT size and mechanical behavior after the linear region. Although the elastic modulus values of the Ni-G-CNT (15,15) structure are the lowest, it has the highest maximum stress value and exhibits a behavior similar to nickel in terms of ductility. The mechanical values of the structures in the CNT direction are given in detail in Table 2.

Table 2. Mechanical properties of the structures under tensile stress in the Z direction.

Models	Elastic Module (GPa)	Yield Strain	Yield Strength (GPa)	Ultimate strain	Ultimate Strength (GPa)
Ni	211,02	0,0368	7,33	0,223	20,96
Ni-G-CNT(5,5)	287,48	0,0349	10,95	0,203	23,34
Ni-G-CNT(10,10)	282,42	0,0346	9,94	0,215	22,31
Ni-G-CNT(15,15)	280,91	0,0331	8,20	0,224	23,47

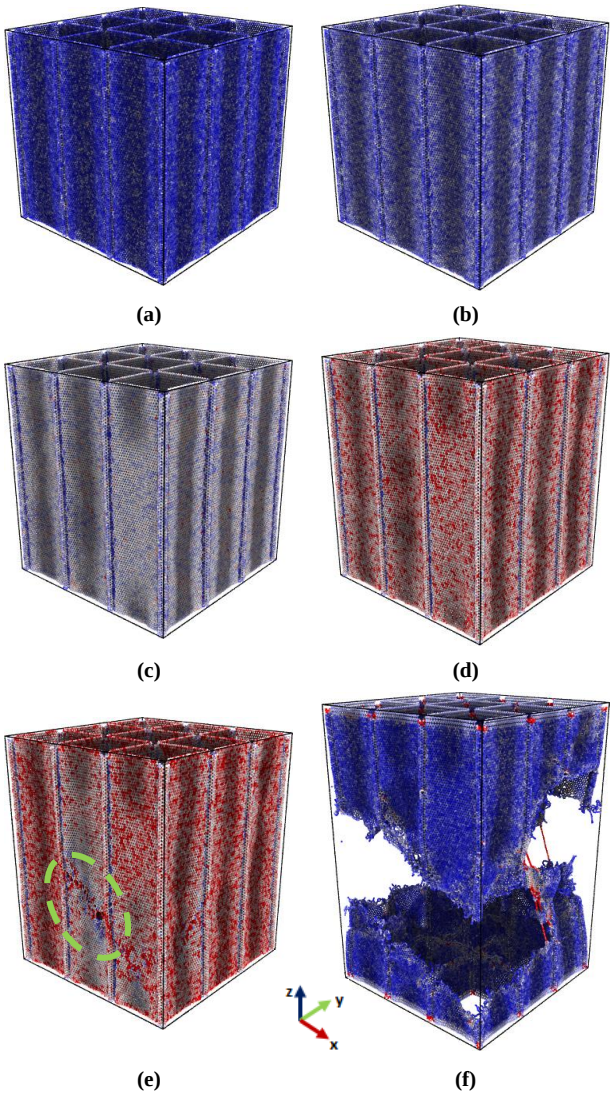

Figure 5. Deformation states of the Ni-G-CNT(5, 5) structure depend on tensile loading perpendicular to the plane, (a) 0.02, (b) 0.06, (c) 0.12, (d) 0.20, (e) 0.22 and (f) 0.44.

In order to better understand the deformation mechanism of Ni-G-CNT structures, the deformation states of an example structure due to tensile loading in the CNT direction are given in Figure 5. When the images are examined, the stresses in the structure gradually increase due to the strain. It has been observed that most of the stresses are concentrated in graphene and CNTs, but nickel material also carries the load. The first rupture deformation occurred at the nickel atoms located at the border between 0.07 and 0.08. For this reason, a decrease in the stress curve is observed. From this point on, stresses accumulate in graphene and CNTs and it is seen that the stresses increase again and reach the maximum value in the 0.20-0.23 strain range. As seen in Figure 5. (e), it was observed that the breaks in this range occurred diagonally from the midpoint of the graphene. Although there was a rapid decrease in stresses after the maximum stress value with the rupture of the ligaments, the stresses continued to increase up to 0.30-0.31ε because the other unruptured graphene and CNT structures continued to carry stress.

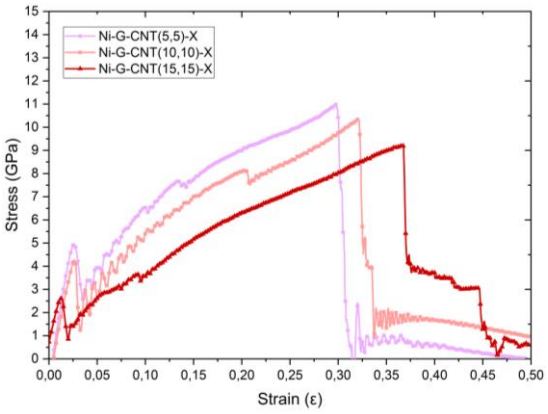

Figure 6. Tensile stress-strain curves of Ni-G-CNT structures in the x direction.

In order to examine the behavior of the structures in the horizontal direction, when the stress strain curves in the transverse direction of CNT of the structures given in Figure 6 are examined, it was observed that the stresses increased linearly, followed by a partial decrease in the stresses and then increased again. It is thought that the reason for the decrease in this first region is due to the flattening of CNTs with circular cross-sections. After the flattening of the CNTs occurred, the stresses increased again and reached the maximum stress value in the range of 0.30-0.37ε and ruptures occurred in the structure. When the mechanical behaviors of different N-G-CNT structures were compared with each other, it was seen that the highest value in this direction belonged to the Ni-G-CNT (5,5) structure and the lowest value belonged to the Ni-G-CNT (15,15) structure. As the CNT diameter increases, the ductility of the material increases, while its elastic modulus, Yield stress and ultimate tensile strength decrease. Table 3 shows the detailed mechanical values of the structures.

Table 3. Mechanical properties of the structures under tensile stress in the X direction.

Models	Elastic Module (GPa)	Yield Strain	Yield Strength (GPa)	Ultimate strain	Ultimate Strength (GPa)
Ni-G-CNT(5,5)	266,73	0,0247	5,14	0,305	11,78
Ni-G-CNT(10,10)	223,74	0,0259	4,74	0,321	11,16
Ni-G-CNT(15,15)	184,69	0,0122	2,59	0,367	9,22

The deformation states obtained for the transverse tensile loading of the Ni-G-CNT(5x5) structure are given in Figure 7. As can be seen from the deformation images, the stresses in the structure increase up to 0.025ε due to the shape change. After this value, it was observed that the stresses decreased and then increased again as flattening occurred in the circular sections of CNTs. The majority of the stresses occur in graphene. After 0.025ε, fluctuating decreases and increases in stress values are observed as the contractions continue in the circular cross-sections of CNTs. The rupture in the structure occurred in the graphene region at values of 0.305, 0.321 and 0.367ε, from small-diameter CNT structures to large ones, respectively. When the tensile strengths of the structures in the transverse direction of CNTs were compared with the nickel structure, it was observed that the tensile strength decreased in this direction but the ductility

increased. It is thought that this decrease is due to two reasons. The first reason may be the fact that CNTs are located in the transverse direction and the flattening of their circular cross-sections. The second reason is that it is thought that nickel atoms exhibit rigid motion and do not contribute to tensile strength due to the division of nickel atoms by the G-CNT cage system.

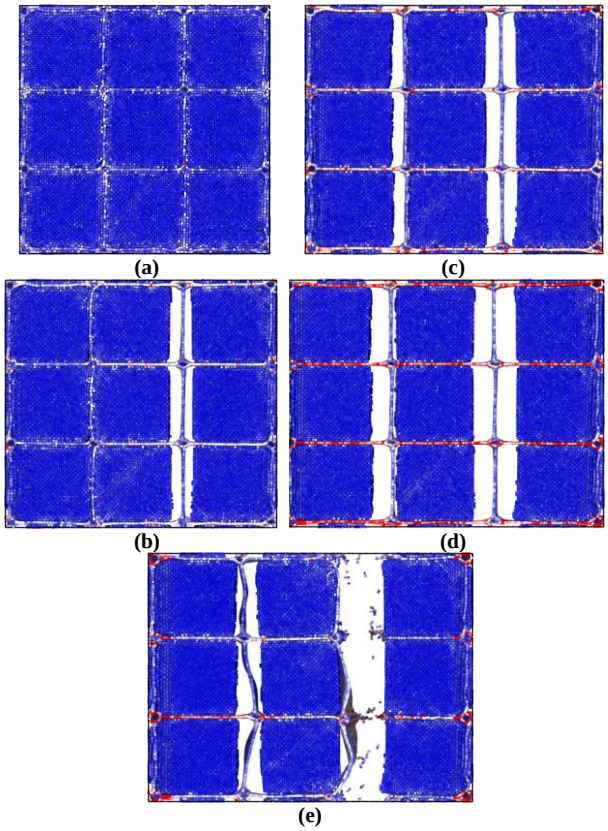

Figure 7. Deformation states of the Ni-G-CNT (5, 5) structure subjected to tensile loading in the transverse direction, (a) 0.00, (b) 0.10, (c) 0.20, (d) 0.30 and (e) 0.31.

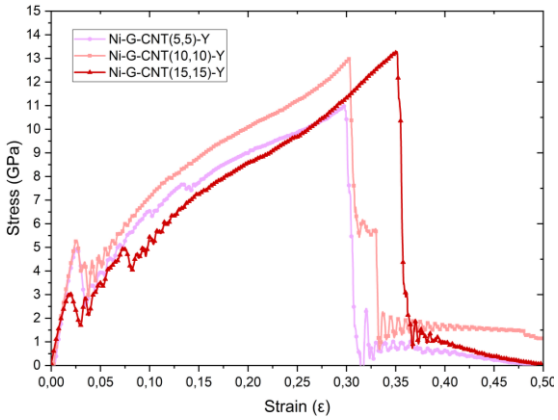

Figure 8. Tensile stress-strain curves of Ni-G-CNT structures in the y direction.

The stress-strain curves of the structures in the y-axis direction are given in Figure 8. When the stress strain curves were examined, it was seen that the behavior was parallel to the x-axis. The stresses increase until the CNT strength is exceeded and then show a partial decrease due to the narrowing in the cross-section. Table 4 gives the mechanical values of the structures in the Y direction.

Table 4. Mechanical properties of the structures under tensile stress in the Y direction.

Models	Elastic Module (GPa)	Yield Strain	Yield Strength (GPa)	Ultimate strain	Ultimate Strength (GPa)
Ni-G-CNT(5,5)	266,73	0,0247	5,14	0,305	11,78
Ni-G-CNT(10,10)	244,75	0,0257	5,29	0,303	13,02
Ni-G-CNT(15,15)	195,46	0,0171	2,81	0,351	13,28

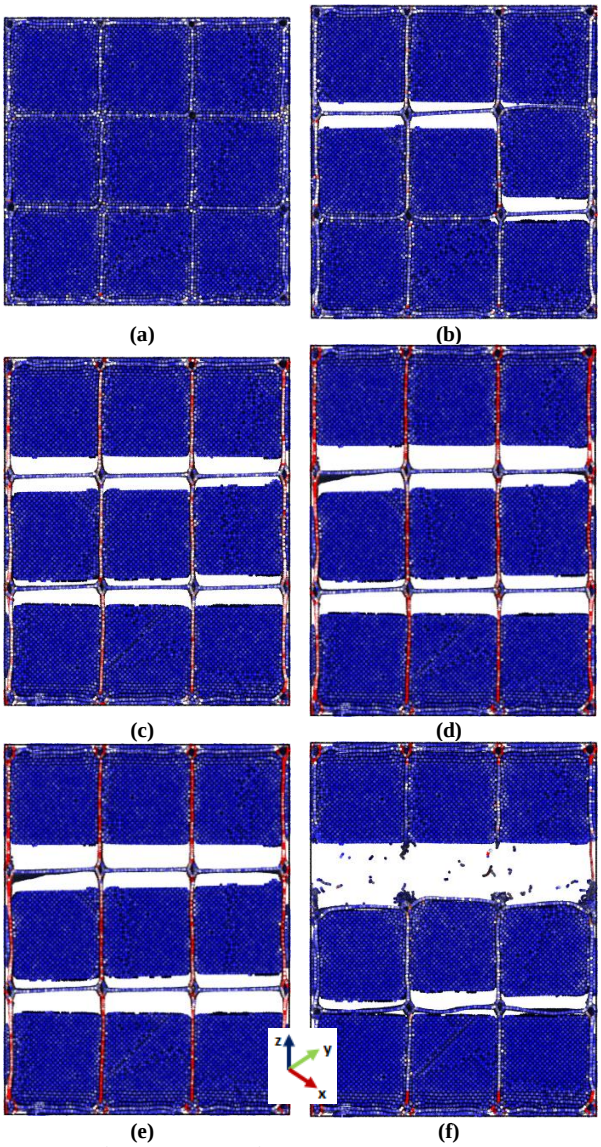

Figure 9. Deformation states of the Ni-G-CNT(5, 5) structure subjected to tensile loading in the Y direction, (a) 0.00, (b) 0.10, (c) 0.16, (d) 0.22, (e) 0.30 and (f) 0.31.

When the values were examined, it was seen that the elastic modulus values decreased as the CNT diameter increased. However, unlike the x direction, the highest maximum stress value and ductility were seen in the Ni-G-CNT (15x15) structure containing CNTs with the largest diameter. It is seen that the tensile strengths of the structures change depending on the number and arrangement of graphene and CNT. Since the Ni-G-CNT(5,5) structure has the same number of graphene and CNTs in both directions, its mechanical strength is the same, while in the other two structures, it is seen that the mechanical strength in the Y direction is higher than in the x direction. This is related to the presence of fewer

CNTs and graphene in the Y direction. In this direction, graphenes is longer and the number of divisions in the nickel structure due to G-CNT connections is less. For this reason, it is thought that the decrease in mechanical values is less. Deformation images of the structures are given in Figure 9. When the deformation images are examined, it is seen that the stresses are mostly concentrated in the graphene, similar to the x direction, and the rupture starts from the graphene in the middle part.

3.1. Compression Behavior

To examine the compression performances of the structure obtained by adding the G-CNT skeleton structure to the Ni structure, the comparative compressive stress-strain curves of different Ni-G-CNT structures are given in Figure 10.

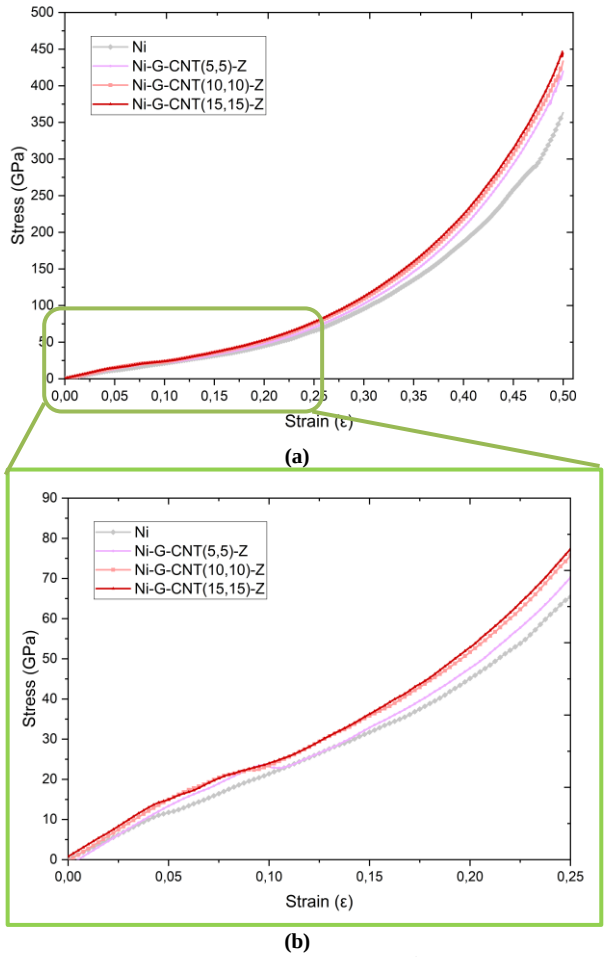

Figure 10. (a) Compressive stress-strain curves of Ni-G-CNT structures in the z direction, (b) zoomed region for 0,00-0,25 strain.

When the behaviors were examined, three different regions were observed. It was observed that in the first region, the stresses in the structure increased linearly up to ε = 0.035-0.050. Then, the slope of the stresses decreases to a certain value. It was observed that after this value, a concentration zone was formed where the stresses increased. Adding G-CNT structures to the structure increased the compressive strength of the nickel material. When the structures were evaluated in terms of CNT dimensions, it was seen that as the diameter of the CNTs increased, up to a certain value in the linear region, the stress values and CNT strengths were higher. Although the increases in this part are low, the stress contribution is more clearly seen in the condensation and hardening region. Detailed mechanical values of the structures are given in table 5.

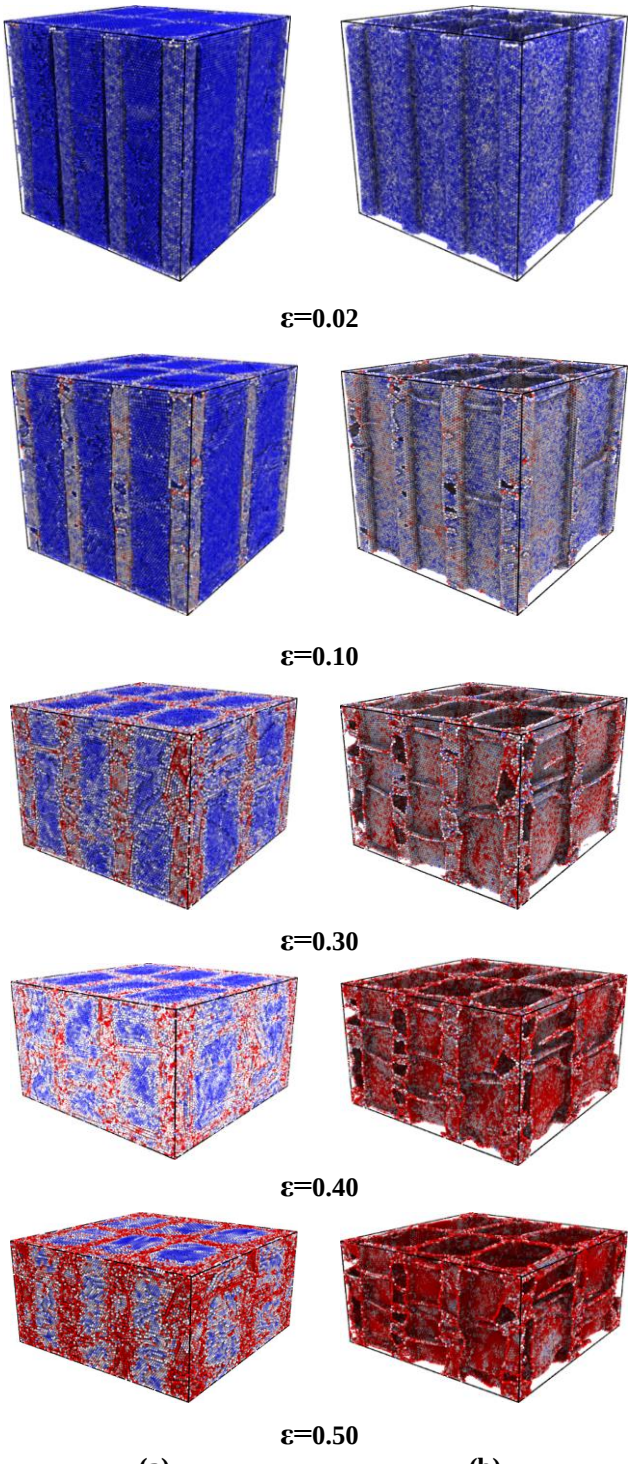

Figure 11. Compressive stress-strain curves in the Z direction of the Ni-G-CNT(15x15) structure, (a) the entire structure, (b) G-CNT skeleton.

Table 5. Mechanical properties of Ni-G-CNT nanomaterials for uniaxial compressive loading.

Model name	Elastic Module (GPa)	Yield strain (%)	Yield Strength (GPa)
Ni	245,67	0,048	11,49
Ni-G-CNT(5,5)	302,33	0,054	14,25
Ni-G-CNT(10,10)	306,15	0,053	16,14
Ni-G-CNT(15,15)	307,65	0,047	14,49

In order to better understand the compression behavior, the stress images of the materials were examined (Figure 11). The first stresses in the structure occurred in graphene and CNTs rather than nickel. It has been observed that as the stresses increase, bending begins in the CNTs and increases up to ε=0.03-0.05. After this value, the slope of the increase in stresses decreases due to lateral deformations occurring in CNTs. In this part, the stresses show a low slope. It was observed that the stresses increased again with an increasing slope starting from ε = 0.10. When the structures with different CNT diameters were examined, in the structures containing large diameter CNTs, the stress was higher in the first region, while this difference became more evident in the concentration region. The highest compressive strength belongs to the Ni-G-CNT(15,15) structure.

4. CONCLUSION

In summary, in this study, a new nanostructure was presented by embedding the carbon-based skeleton structure created by covalently bonding Graphene and CNT together into nickel metal. After checking the thermodynamic stability of the structures, mechanical analyzes were performed using MD simulations. The results showed that strong covalent bonds were formed between graphene and CNT structures and a structure exhibiting higher elastic modulus, ultimate strength and strain values in the vertical direction was obtained compared to the Ni structure. With the addition of G-CNT structures, a 36% increase in the elastic modulus of the nickel structure and a 12% increase in the maximum tensile value were observed. The structure inherently exhibits an anisotropic behavior. Additionally, when the effects of different CNT diameters on the mechanical strength of the structure were investigated, it was seen that larger diameter CNTs were better in compressive strength in the vertical direction. The situation may differ in tensile strength. With this study, an important G-CNT structure reinforcement has been presented to improve the low mechanical strength of nickel material, which has unique properties such as rust resistance, high temperature, electrical conductivity and chemical resistance.

Declaration of conflicting interests

The authors declared no potential conflicts of interest with respect to the research, authorship, and/or publication of this article.

REFERENCES

[1] U. Degirmenci, Y.O. Yildiz, Examination of mechanical behaviour of fullerene doped aluminium matrix composite produced by sintering process, Materials Today Communications 38 (2024) 107916.

[2] J. Xu, J. Tao, S. Jiang, Z. Xu, Investigation on corrosion and wear behaviors of nanoparticles reinforced Ni-based composite alloying layer, Applied Surface Science 254(13) (2008) 4036-4043.

[3] L. Zhang, D. Shi, T. Liu, M. Jaroniec, J. Yu, Nickel-based materials for supercapacitors, Materials Today 25 (2019) 35-65.

[4] Y. Li, J. Zhang, Z. Chen, M. Chen, Nickel-based materials: Toward practical application of the aqueous hybrid supercapacitors, Sustainable Materials and Technologies 33 (2022) e00479.

[5] B. Li, M. Zheng, H. Xue, H. Pang, High performance electrochemical capacitor materials focusing on nickel based materials, Inorganic Chemistry Frontiers 3(2) (2016) 175-202.

[6] Y. Zhou, W.-G. Jiang, D.-S. Li, Q.-H. Qin, Study on Lightweight and Strengthening Effect of Carbon Nanotube in Highly Ordered Nanoporous Nickel: A Molecular Dynamics Study, Applied Sciences, 2019.

[7] M. Dadkhah, A. Saboori, P. Fino, An Overview of the Recent Developments in Metal Matrix Nanocomposites Reinforced by Graphene, Materials, 2019.

[8] M. Tabandeh-Khorshid, K. Ajay, E. Omrani, C. Kim, P. Rohatgi, Synthesis, characterization, and properties of graphene reinforced metal-matrix nanocomposites, Composites Part B: Engineering 183 (2020) 107664.

[9] C. Qiu, Y. Su, J. Yang, B. Chen, Q. Ouyang, D. Zhang, Structural modelling and mechanical behaviors of graphene/carbon nanotubes reinforced metal matrix composites via atomic-scale simulations: A review, Composites Part C: Open Access 4 (2021) 100120.

[10] B. Guo, B. Chen, X. Zhang, X. Cen, X. Wang, M. Song, S. Ni, J. Yi, T. Shen, Y. Du, Exploring the size effects of Al4C3 on the mechanical properties and thermal behaviors of Al-based composites reinforced by SiC and carbon nanotubes, Carbon 135 (2018) 224-235.

[11] D. Kuang, L. Xu, L. Liu, W. Hu, Y. Wu, Graphene–nickel composites, Applied Surface Science 273 (2013) 484-490.

[12] N. Wang, S. Pandit, L. Ye, M. Edwards, V.R.S.S. Mokkapati, M. Murugesan, V. Kuzmenko, C. Zhao, F. Westerlund, I. Mijakovic, J. Liu, Efficient surface modification of carbon nanotubes for fabricating high performance CNT based hybrid nanostructures, Carbon 111 (2017) 402-410.

[13] S. Inoue, Y. Matsumura, Influence of metal coating on single-walled carbon nanotube: Molecular dynamics approach to determine tensile strength, Chemical Physics Letters 469(1) (2009) 125-129.

[14] S. Inoue, Y. Matsumura, Molecular dynamics simulation of metal coating on single-walled carbon

nanotube, Chemical Physics Letters 464(4) (2008) 160-165.
[15] J. Jiang, J. Liu, W. Zhou, J. Zhu, X. Huang, X. Qi, H. Zhang, T. Yu, CNT/Ni hybrid nanostructured arrays: synthesis and application as high-performance electrode materials for pseudocapacitors, Energy & Environmental Science 4(12) (2011) 5000-5007.
[16] D. Wang, X. Wang, L. Qiu, H. Ye, N. Maimaitituersun, B. Han, Effect of nickel-coated carbon nanotubes on the tensile behaviors of ultra-high performance concrete (UHPC): insights from experiments and molecular dynamic simulations, Journal of Materials Science 58(45) (2023) 17225-17240.
[17] K. Duan, L. Li, Y. Hu, X. Wang, Enhanced interfacial strength of carbon nanotube/copper nanocomposites via Ni-coating: Molecular-dynamics insights, Physica E Low Dimens. Syst. Nanostruct. 88 (2017) 259-264.
[18] P.K. Singh, K. Sharma, A. Kumar, M. Shukla, Effects of functionalization on the mechanical properties of multiwalled carbon nanotubes: A molecular dynamics approach, Journal of Composite Materials 51(5) (2016) 671-680.
[19] H. Y. Song, X.-W. Zha, Mechanical properties of nickel-coated single-walled carbon nanotubes and their embedded gold matrix composites, Physics Letters A 374(8) (2010) 1068-1072.
[20] Y. Yan, A. Zou, Y. Lei, P. Xu, S. Zhou, Atomic insights into the tensile behavior of carbon nanotube with different geometrical characteristics embedded in nickel matrix, Diamond and Related Materials 141 (2024) 110576.
[21] W. Humphrey, A. Dalke, K. Schulten, VMD: Visual molecular dynamics, Journal of Molecular Graphics 14(1) (1996) 33-38.
[22] F.Y. Meng, S.Q. Shi, D.S. Xu, R. Yang, Size effect of X-shaped carbon nanotube junctions, Carbon 44(7) (2006) 1263-1266.
[23] U. Degirmenci, M. Kirca, Design and mechanical characterization of a novel carbon-based hybrid foam: A molecular dynamics study, Comput. Mater. Sci. 154 (2018) 122-131.
[24] S. Plimpton, Fast Parallel Algorithms for Short-Range Molecular Dynamics, Journal of Computational Physics 117(1) (1995) 1-19.
[25] U. Degirmenci, M. Kirca, Carbon-based nano lattice hybrid structures: Mechanical and thermal properties, Physica E Low Dimens. Syst. Nanostruct. 144 (2022) 115392.
[26] S.K. Deb Nath, S.-G. Kim, Study of the Nanomechanics of CNTs under Tension by Molecular Dynamics Simulation Using Different Potentials, ISRN Condensed Matter Physics 2014 (2014) 606017.
[27] M.S. Daw, M.I. Baskes, Embedded-atom method: Derivation and application to impurities, surfaces, and other defects in metals, Physical Review B 29(12) (1984) 6443-6453.
[28] X.-M. Bai, A.F. Voter, R.G. Hoagland, M. Nastasi, B.P. Uberuaga, Efficient Annealing of Radiation Damage Near Grain Boundaries via Interstitial Emission, Science 327(5973) (2010) 1631-1634.
[29] Y.-H. Lin, T.-C. Chen, P.-F. Yang, S.-R. Jian, Y.-S. Lai, Atomic-level simulations of nanoindentation-induced phase transformation in mono-crystalline silicon, Applied Surface Science 254(5) (2007) 1415-1422.
[30] S.-P. Huang, D.S. Mainardi, P.B. Balbuena, Structure and dynamics of graphite-supported bimetallic nanoclusters, Surface Science 545(3) (2003) 163-179.
[31] Y. Shibuta, S. Maruyama, Bond-order potential for transition metal carbide cluster for the growth simulation of a single-walled carbon nanotube, Comput. Mater. Sci. 39(4) (2007) 842-848.
[32] M. Kirca, X. Yang, A.C. To, A stochastic algorithm for modeling heat welded random carbon nanotube network, Computer Methods in Applied Mechanics and Engineering 259 (2013) 1-9.
[33] A.P. Thompson, S.J. Plimpton, W. Mattson, General formulation of pressure and stress tensor for arbitrary many-body interaction potentials under periodic boundary conditions, The Journal of Chemical Physics 131(15) (2009) 154107.